An Effective Level Set-based Method for the Design of Extrudable Structures

H. Li[1], *L. Gao[1], P.G. Li[1] and T. Wu[2]

[1] School of Mechanical Science & Engineering, Huazhong University of Science and Technology, China
[2] School of Software Engineering, Huazhong University of Science and Technology, China

*Corresponding author: gaoliang@mail.hust.edu.cn

Abstract

Extrusion is a manufacturing technique that creates products with constant cross sections. The extrusion process is widely employed to reduce cost. The conventional structure optimization approaches are typically failed to deal with this particular manufacture constraint. Therefore, this paper presents an effective level set method for the optimal design of structures with extrusion constraint. The free boundary of the structure is embedded into a higher-dimensional level set function, which can be used to implement the structural shape and topology optimization simultaneously. The compactly supported radial basis functions (CS-RBFs) are introduced to convert the conventional level set method to an easier parameterization form. Discrete wavelets transform (DWT) approximation is utilized to produce a sparser linear system to accelerate the fitting and evaluation operations arise from the parametric formulation. Furthermore, a cross section projection strategy is applied to reduce the design variables and satisfy the extrusion constraint. Several numerical examples are provided.

Keywords: Level set method, Radial basis functions, Parameterization, Discrete wavelets transform, Extrusion constraint purposes.

Introduction

Manufacturing significantly influences the cost in a product. The extrusion process is introduced to be an effective technique to reduce the cost of production. In the extrusion manufacturing process, materials are squeezed through an orifice of the required shape in a die by using the pressure from a ram. The primary fact of enforcing this process is to keep the same cross-sections along the extrusion path. It is suggested that one should take care of the manufacturing issues in the early stage of the design cycle, in order to save the development costs and shorten the research time.

Structural topology optimization is identified as one of the most effective tools for improving the performance of structures. This topic has experienced remarkable progress in various engineering areas during the past decades (Bendsøe and Kikuchi, 1988; Rozvany, 2008). Nevertheless, these research works are mainly focused on optimizing the structural performance, and only a few amounts of them consider the other aspect in the design of structures – manufacturing. For an extrudable product, it means that we must simultaneously optimize the performance of a structure and guarantee the structure has the constant geometries along the fixed path to satisfy the extrusion constraint.

Several studies have been made for solving the optimization problems with extrusion constraints. Kim and Kim (2000) were among the earliest researchers who studied the topology optimization of beam cross-section. Zhou et al. (2002) proposed the mathematical formulation for the topology optimization with extrusion constraint, which is embedded in the software Optistruct. Ishii and Aomura (2004) utilized the homogenization method to solve the extrusion-based structural optimization problem. Liu et al. (2007) solved the beam cross-sectional optimization problems considering warping of sections and coupling among deformations by using the SIMP-based approach. Patel et al. (2009) proposed a methodology by using the hybrid cellular automaton method to handle the extrusion-based nonlinear transient design problems. Zuberi et al. (2009) investigated the influence of different configuration and location of the boundary conditions on the optimal results for the extrudable designs.

In this study, we present an effective parametric level set method for the design of extrudable structures. The DWT is incorporated into the CSRBF-based level set formulation to achieve an extremely sparse linear system for the interpolation. It transforms the collection matrix into a wavelet basis, and then compresses this matrix with very few nonzero elements via thresholding. The extrusion constraint is satisfied by an elaborated strategy called cross section projection.

Implicit free boundary representation

The level set method implicitly models the motion of free boundary of a structure via the Lipschitz-continuous scalar function, and the structural boundary can be interpreted by the zero iso-surface of the one-higher dimensional level set function. Assume that $\Omega \subset R^d\,(d = 2or3)$ is the space occupied by a structure, each part of the domain can be defined with the level set function as:

$$\begin{cases} \Phi(\mathbf{x}) > 0 \Leftrightarrow \forall \mathbf{x} \in \Omega \setminus \partial\Omega & \text{(solid)} \\ \Phi(\mathbf{x}) = 0 \Leftrightarrow \forall \mathbf{x} \in \partial\Omega \cap D & \text{(boundary)} \\ \Phi(\mathbf{x}) < 0 \Leftrightarrow \forall \mathbf{x} \in D \setminus \Omega & \text{(hole)} \end{cases} \tag{1}$$

where D is a pre-defined design domain where all admissible shapes Ω are included, i.e. $\Omega \subseteq D$.

In order to dynamically drive the free boundary, introducing the pseudo-time t into the level set function leads to following first-order Hamilton-Jacobi PDE:

$$\frac{\partial \Phi(\mathbf{x},t)}{\partial t} + \mathbf{v_n}(\mathbf{x})\left|\nabla\Phi(\mathbf{x},t)\right| = 0, \qquad \Phi(\mathbf{x},0) = \Phi_0(\mathbf{x}) \tag{2}$$

where $\mathbf{v_n}(\mathbf{x})$ is the normal velocity associated with the sensitivity of the objective function with respect to the boundary variation. Moving the structural boundary $\Phi(\mathbf{x},0)$ along the normal direction $\mathbf{n}$ is equivalent to update the values of level set function via solving the Hamilton-Jacobi PDE with proper numerical schemes.

An important issue of the conventional level set method is that the explicit analytical form of the level set function is unknown. As a result, to solve the Hamilton-Jacobi PDE on the fixed Eulerian grids and obtain the discrete level set values, one should conquer the numerical difficulties in handling the complicated PDEs, including the CFL condition, re-initializations of level-set surface and velocity extensions (Wang, Wang et al., 2003; Allaire, Jouve et al., 2004).

Level set parameterization

To overcome the unfavorable numerical features in the standard level set method, the parametric level set formulation has been developed as an alternative. In this paper, the CSRBFs are used to parameterize the level set-based optimization model. The CSRBF is a kind of radial symmetrically function centered at a particular knot with compact support (Wendland, 2006), which is widely applied to interpolate massive scatter data. Comparing with the globally supported kernels or the piecewise polynomials, the CSRBFs have several attractive features, such as strictly definiteness, sparseness of interpolant matrix, desirable smoothness of the partial derivatives and so on.

Here, we adopt the CSRBF with C2 continuity of Wendland' series, in that it can be utilized to interpolate the level set function with favorable smoothness and desired completeness when the knots are dense enough (Luo, Wang et al., 2008). The Wendland function with C2 continuity, whose shapes are plotted in Fig. 1, is given as follows:

$$\psi(r) = \max\left\{0,(1-r)^4\right\}(4r+1) \tag{3}$$

and its derivatives in the X and Y direction are stated respectively as:

$$\frac{\partial\psi}{\partial x} = \frac{\partial\psi}{\partial r}\frac{\partial r}{\partial x} = \max\left\{0,(1-r)^3(-20r)\frac{\partial r}{\partial x}\right\} \tag{4}$$

$$\frac{\partial\psi}{\partial y} = \frac{\partial\psi}{\partial r}\frac{\partial r}{\partial y} = \max\left\{0,(1-r)^3(-20r)\frac{\partial r}{\partial y}\right\} \tag{5}$$

where r is the radius of support, which is defined in a 2D Euclidean space as:

$$r = \frac{d_I}{R} = \frac{\sqrt{(x-x_i)^2+(y-y_i)^2}}{R} \tag{6}$$

The parameter R is introduced to determine the compact support size at each knot. It is suggested that a too small radius may lead to singular stiffness matrix, and a too large radius would obviously increase the computation time. Therefore, an experiential criterion in selecting a radius of support is used (Luo, Tong et al., 2009).

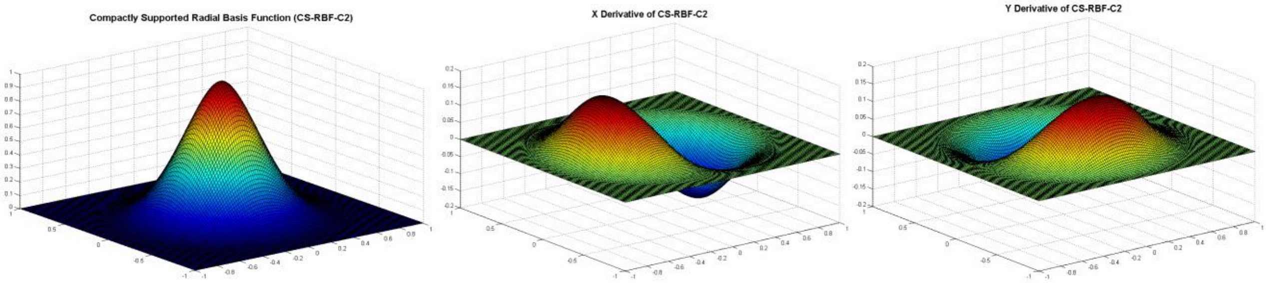

(a) **(b)** **(c)**

Figure 1. CSRBF with C2 continuity and its derivatives: (a) shape of CSRBF; (b) X derivative of CSRBF; (c) Y derivative of CSRBF.

Now, we aim at interpolating the level set function with the CSRBFs. For simplicity, the level set grids are assumed to be identical with the meshes for finite element analysis, which are consisting of N individual nodes or knots. For the CSRBF kernels, we rewrite them in the vector form as:

$$\boldsymbol{\psi}(\mathbf{x}) = [\psi_1(\mathbf{x}), \psi_2(\mathbf{x}), ..., \psi_N(\mathbf{x})]^{\mathrm{T}} \in \mathbb{R}^{\mathrm{N}} \tag{7}$$

and the expansion coefficients served as the design variables are given as:

$$\boldsymbol{\alpha}(\mathbf{t}) = [\alpha_1(t), \alpha_2(t), ..., \alpha_N(t)]^{\mathrm{T}} \in \mathbb{R}^{\mathrm{N}} \tag{8}$$

It is obviously that the coefficients $\boldsymbol{\alpha}$ are time-dependent, and the CSRBFs are only space-dependent. The originally coupled level set function can be separated of time and space by the product of a matrix and a vector:

$$\boldsymbol{\Phi} = \mathbf{A}\boldsymbol{\alpha}, \text{ where } \boldsymbol{\Phi} = \left[\Phi_1, \Phi_2, ..., \Phi_N\right]^{\mathrm{T}} \tag{9}$$

In Equation (8), the matrix $\mathbf{A}$ is theoretically invertible, and can be expressed as:

$$\mathbf{A} = \begin{bmatrix} \boldsymbol{\psi}^{\mathrm{T}}(x_1) \\ \boldsymbol{\psi}^{\mathrm{T}}(x_2) \\ \cdots \\ \boldsymbol{\psi}^{\mathrm{T}}(x_N) \end{bmatrix} = \begin{bmatrix} \psi_1(x_1) & \psi_2(x_1) & \cdots & \psi_N(x_1) \\ \psi_1(x_2) & \psi_2(x_2) & \cdots & \psi_N(x_2) \\ \cdots & \cdots & \cdots & \cdots \\ \psi_1(x_N) & \psi_2(x_N) & \cdots & \psi_N(x_N) \end{bmatrix} \tag{10}$$

It should be pointed out that for the initialization of the optimization, one must, firstly, solve the following system to obtain the initial value of expansion coefficients:

$$\boldsymbol{\alpha} = \mathbf{A}^{-1}\boldsymbol{\Phi}_0 \tag{11}$$

where $\boldsymbol{\Phi}_0$ are the pre-determined discrete level set values before the iteration.

With regard to the Hamilton-Jacobi PDE, it can be rewritten with the CSRBF approximation as:

$$\boldsymbol{\psi}^{\mathrm{T}}(\mathbf{x})\frac{d\boldsymbol{\alpha}(t)}{dt} + \mathbf{v_n}\,|\nabla\boldsymbol{\psi}^{\mathrm{T}}(\mathbf{x})\boldsymbol{\alpha}(t)| = 0 \tag{12}$$

Hereto, the conventional level set method has been converted into a parametric one without losing any of its favorable characteristics, and the well-established gradient-based approaches can be conveniently applied to deal with the parameterization formulation.

Matrix compression

In this section, we discuss the large-scale linear system arisen from the RBF interpolant. Let us consider the Eq. (9) and (11). It is easy to notice that for the large system, especially with the 3D structural optimization problems, more zeros in the matrix $\mathbf{A}$ means less computational cost as well as less computer storage for solving the system. We can expect that CSRBFs will somewhat reduce the impediments caused by the fully dense matrix, but it is not satisfied. Here, a DWT-based matrix compression technique is introduced to produce much sparser linear system.

DWT is worked as fast linear operation acting on a data vector or matrix, and transforms it into a numerically disparate vector or matrix with the wavelet basis. The new vector or matrix is always of the same size with the original one. This technique has been successfully implemented in the field of image/video processing, signal analysis, computer vision and so on (Mallat, 1989). In recent years, it application has been extended into solving the fully populated linear system (Chen, 1999; Ravnik, Škerget et al., 2004).

In this paper, the Haar wavelet is adopted due to its non-overlapping support and constant scaling function (Ravnik, Škerget et al., 2004). To facilitate the discussion, we introduce the **W** matrix that is defined in previous work by the authors (Chen, 1999; Ford and Tyrtyshnikov, 2003). The orthogonal matrix **W** can be used to convert the vector from the standard basis to the wavelet basis. Considering the three components within the system defined in Eq. (9), we can transform the vectors into wavelet forms as:

$$\bar{\boldsymbol{\alpha}} = \mathbf{W} \cdot \boldsymbol{\alpha} \tag{13}$$

$$\bar{\boldsymbol{\Phi}} = \mathbf{W} \cdot \boldsymbol{\Phi} \tag{14}$$

and the matrix can be given as:

$$\bar{\mathbf{A}} = \mathbf{W} \cdot \mathbf{A} \cdot \mathbf{W}^{\mathrm{T}} \tag{15}$$

From Eq. (9) we get

$$\mathbf{W} \cdot \mathbf{A} \cdot \left(\mathbf{W}^{\mathrm{T}} \cdot \mathbf{W}\right) \cdot \boldsymbol{\alpha} = \mathbf{W} \cdot \boldsymbol{\Phi} \tag{16}$$

Substituting Eq. (13)-(15) into Eq. (16), it yields:

$$\bar{\mathbf{A}} \cdot \bar{\boldsymbol{\alpha}} = \bar{\boldsymbol{\Phi}} \tag{17}$$

Since the elements in original matrix **A** have smoothly variational values, there are only a few important coefficients in the wavelet representation $\bar{\mathbf{A}}$. In other words, we can zero out the elements with redundant information in $\bar{\mathbf{A}}$ by means of hard thresholding. In this study, we determine the adaptive threshold using the scheme described in the work by Ravnik et al. (2004) , and eliminate the non-zero elements with the absolute values less than the threshold.

Therefore, an extremely sparse system consisting of matrix $\bar{\mathbf{A}}^*$ is obtained after denoising:

$$\bar{\mathbf{A}}^* \cdot \bar{\boldsymbol{\alpha}} = \bar{\boldsymbol{\Phi}} \tag{18}$$

Eventually, the value of level set function and expansion coefficients can be determined by the reconstruction operator as:

$$\boldsymbol{\alpha} = \mathbf{W}^{\mathrm{T}} \cdot \bar{\boldsymbol{\alpha}} \text{ or } \boldsymbol{\Phi} = \mathbf{W}^{\mathrm{T}} \cdot \bar{\boldsymbol{\Phi}} \tag{19}$$

It is expected that incorporating DWT-based scheme into CSRBF interpolation can produce an easily-solved linear system with much less computational cost and computer storage.

Extrusion based optimization design

In this section, we take the minimum strain energy problem considering the extrusion constraint as an example. Generally, if an extrudable design is required, one must ensure that the cross-sections along a specified path are kept constant. Regarding the level set-based approach, it means the discrete level set values at the corresponding knots within the structural cross sections must be identical to maintain the same level set surface along the extrusion path. Thus, the extrusion-based compliance optimization problem is established as:

$$
\begin{aligned}
&\underset{(u,\Phi)}{Minimize}: J(u,\Phi)=\int_D f(u)H(\Phi)d\Omega \\
&Subject\ \ to: a(u,v,\Phi)=l(v,\Phi), \forall v\in U,\ u\big|_{\partial\Omega}=u_0 \\
&\qquad\qquad G(u,\Phi)=\int_D H(\Phi)d\Omega-V_{\max}\le 0 \\
&\qquad\qquad \left(\Phi_i=\Phi_j=...=\Phi_{ne}\right)_k,\ k=1,2,...,K
\end{aligned}
\tag{20}
$$

where J is the objective function and G is the global volume constraint with an upper bound of $V_{\max}$, respectively. H is the Heaviside function associated with the implicit level set Φ. K denotes the number of elements in a single cross section, and ne represents the number of elements along the path of the extrusion. The main problem in this formulation is that too many extra constraints are introduced, which will cause complicated solving scheme and exorbitant computational effort.

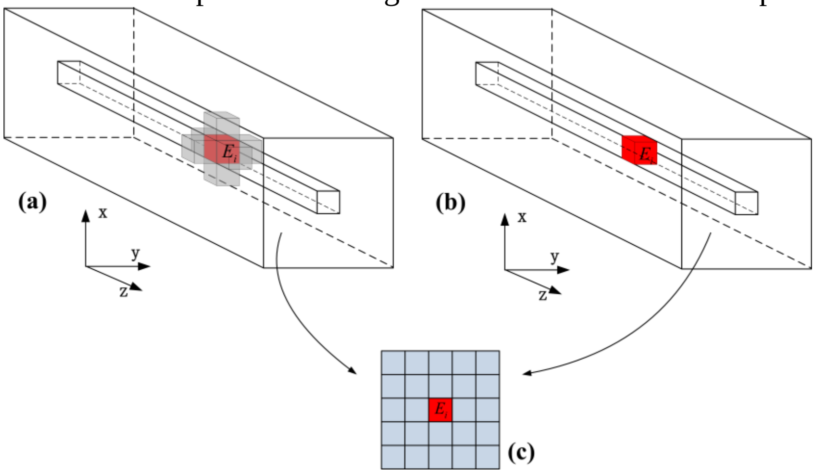

Figure 2. The cross section projection strategy: (a) the adjacent elements; (b) the parallel elements; (c) the projection plane.

As a result, we propose the cross section projection strategy to model the structural optimization problem with extrusion constraint. In the presented method, we aim at mapping the elements in 3D space to a relative 2D projected plane shown in Fig. 2. Generally, we consider two types of elements in the 3D FE model, i.e. the adjacent elements and the parallel elements. The adjacent elements are defined as the elements in a fixed neighborhood of individual element E_i, and the parallel elements are considered as the elements along the same extrusion axis of element E_i. To implement the cross section projection strategy, we must aggregate the influences from the above-mentioned two types of elements to E_i via two specified operation.

For the bilinear functional, we firstly handle the influence from adjacent elements:

$$
\begin{gathered}
\bar{a}(u,v,\Phi)_i=\frac{1}{\sum_{j=1}^{nae} w(i,j)}\sum_{j=1}^{nae}\left[w(i,j)\left(\int_{D_{Ei}}\left(\varepsilon(v_i)\right)^T C(E_i)\varepsilon(u_i)H(\Phi_i)d\Omega_{Ei}\right)\right], \\
w(i,j)=rd-dist(i,j)
\end{gathered}
\tag{21}
$$

and then the influence from the parallel elements:

$$
a_P(u,v,\Phi)=\sum_{k=1}^{K}\left\{\sum_{i=1}^{ne}\bar{a}(u,v,\Phi)_i/ne\right\}_k \tag{22}
$$

In Equation (21) and (22), Ω_{Ei} is the sub-domain occupied by element E_i. $w(i,j)$ is the weight coefficient determined by the radius of neighborhood and the distance between the relatively adjacent elements, i.e. rd and $dist(i,j)$. nae represents the number of adjacent elements within radius rd.

Similarly, the loading functional is given by the aforementioned two steps:

$$\bar{l}(v,\Phi)_i = \frac{1}{\sum_{j=1}^{nae} w(i,j)} \sum_{j=1}^{nae} \left[w(i,j) \left(\int_{D_{Ei}} pvH(\Phi_i) d\Omega_{Ei} + \int_{\Gamma_{Ei}} \tau vHd\Gamma_{Ei} \right) \right] \tag{23}$$

$$l_P(v,\Phi) = \sum_{k=1}^{K} \left\{ \sum_{i=1}^{ne} \bar{l}(v,\Phi)_i / ne \right\}_k \tag{24}$$

Hereto, the new model for extrusion-based topology optimization can be stated as:

$$\begin{aligned} &\underset{(u,\Phi)}{Minimize}: J_P(u,\Phi) = \int_{D_P} f(u) H(\Phi) d\Omega_P \\ &Subject\ \ to: a_P(u,v,\Phi) = l_P(v,\Phi), \forall v \in U_P,\, u\big|_{\partial\Omega_P} = u_0 \\ &G_P(u,\Phi) = \int_{D_P} H(\Phi) d\Omega_P - V_{\max} \le 0 \end{aligned} \tag{25}$$

We remark that in Eq. (25), there are no manufacturing constraints explicitly existing. Further, since that the search space of the optimization is within a 2D domain, we only need to update a reduced set of design variables with the global volume constraint. However, a 3D finite element analysis is still needed to measure the performance of the entire structure.

Numerical examples

In this section, the proposed method is applied to two 3D examples. The well-established optimality criteria (OC) method (Luo, Tong et al., 2009) is utilized as a numerical solution for these structural compliance optimization problems. The iteration is terminated when the prescribed tolerance TOL=10^{-2} for the difference of two successive objective values is achieved, or the maximum iteration T=200 is reached. It is noted that all the computations are done with MATLAB, and are processed in a computer configured with a CPU 2.67 GHz processor as well as a 4 GB RAM.

We assume that the Young's modulus for solid material is 180GPa and for void material is 0.001Pa. The Possion's ratio for the elastic material is 0.3. The 'ersatz material' model is adopted to evaluate the strain energies on the discontinued boundary without remeshing.

We consider the minimum compliance problem for a 3D structure, shown in Fig. 3. The design domain is a beam of size 0.3m×0.4m×1.2m with the two edges at the bottom face being fixed as the Dirichlet boundary. An external force F=400kN loaded at the center of the top face along the y axis is defined as the non-homogeneous Neumann boundary. The limit of material usage is set to 35% in volume fraction. The radius of support for CSRBF is 3.5. For the finite element analysis, we discretize the entire structure with 12×16×48 tri-linear 8-node cube elements.

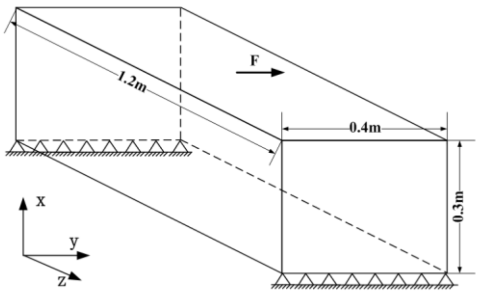

Figure 3. The 3D design domain

In the first example, the optimization problem is solved without considering extrusion constraint. We use the improved parametric level set method to model the 3D structure design problem. The percentage of zero elements in above-mentioned matrix **A**, whose size is 10829×10829, is 98.86%. In other words, only a few nonzero elements are needed to give a good enough approximation of the entire level set surface. Fig. 4(a)-(d) show the evolution of structural boundary. It should be noticed that several regular holes are added factitiously into the rectangular solid in order to speed up the optimization process, and the optimal design achieved by shape fidelity and topological changes via deleting the voids and adding new voids inside the design domain. It is obviously that the final design shown in Fig. 4(d) cannot be fabricated by the extrusion process.

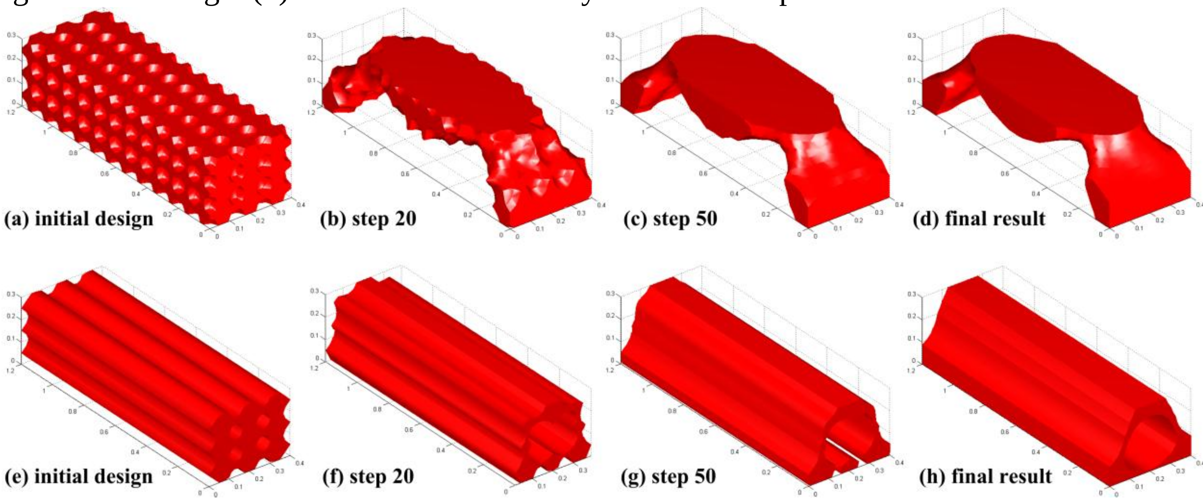

Figure 4. Process of the optimization: (a)-(d) optimization without the extrusion constraint; (e)-(h) optimization with the extrusion constraint.

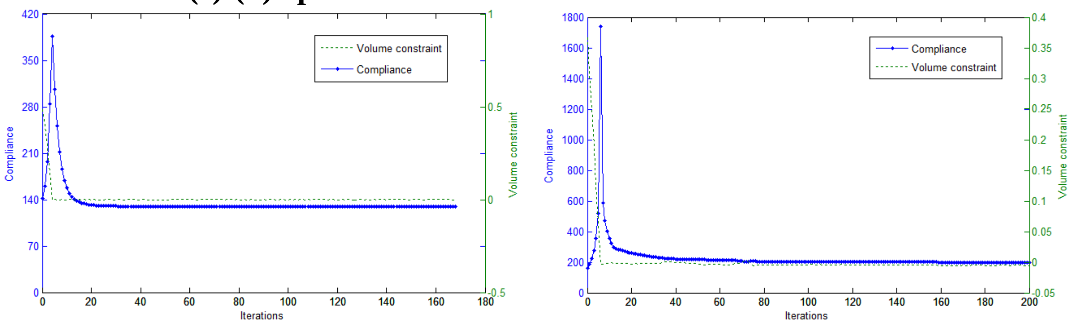

(a) **(b)**

Figure 5. Convergence histories: (a) without extrusion constraint; (b) with extrusion constraint.

In the second example, we consider the design problem with extrusion constraint. We assume that the extrusion path is along the Z axis, and the process of optimization can be seen in Fig. 4(e)-(h). We remark that the initial design (shown in Fig. 4(e)) is quite different from that in the first example, which contains several holes penetrating the entire structure along the extrusion direction to maintain the uniform cross section from the very beginning. Comparing to the first example, the cross-sections in this example are always kept constant during iteration, due to that the optimization is only applied to a 2D projected domain. The optimal design shown in Fig. 4(h) can be manufactured by the extrusion technique along the Z axis.

The iterative histories for the two examples are given in Fig. 5. It takes 167 steps to complete the optimization for the first example, and 200 steps to achieve the optimal design for the second example. The optimal results for the two examples are 129.65 and 197.79, respectively. The compliance in the case without extrusion constraint is smaller than that of the extrusion-based case, in that the manufacturing constraint will reduce the flexibility in the distribution of materials. Moreover, the CPU time of the problem with extrusion constraint is approximately 175.48s per step, which is much less than that of the first example (230.51s per step). It is because that the proposed cross section projection strategy reduces the numbers of design variables to a great extent.

Conclusions

In this study, an effective level set-based parameterization method has been proposed for 3D structures with extrusion constraint. The DWT scheme is incorporated into the CSRBF-based parametric level set model to produce an extremely sparse system. The numerical stability and volume conservative prove its effectiveness. A cross section projection strategy is developed to convert the extrusion-based 3D structure optimization to the 2D issue with fewer numbers of design variables. Two numerical examples in 3D are provided. The numerical results show that the final design can be manufactured by the extrusion process.

Acknowledgments

This work is supported by the National Natural Science Foundation of China (Grant No. 51175197) and the Open Research Fund Program (No. 31115020) of the State Key Laboratory of Advanced Design and Manufacturing for Vehicle Body, Hunan University, China.

References

Allaire, G., Jouve, F. and Toader, A. M. (2004), Structural optimization using sensitivity analysis and a level-set method. *Journal of Computational Physics*, 194(1), pp. 363-393.

Bendsøe, M. P. and Kikuchi, N. (1988), Generating optimal topology in structural design using a homogenization method. *Computer Methods in Applied Mechanics and Engineering*, 71, pp. 197-224.

Chen, K. (1999), Discrete wavelet transforms accelerated sparse preconditioners for dense boundary element systems. *Electronic Transaction Numerical Analysis*, 8, pp. 138-153.

Ford, J. M. and Tyrtyshnikov, E. E. (2003), Combining Kronecker product approximation with discrete wavelet transforms to solve dense, function-related linear systems. *SIAM Journal on Scientific Computing*, 25(3), pp. 961-981.

Ishii, K. and Aomura, S. (2004), Topology optimization for the extruded three dimensional structure with constant cross section. *JSME International Journal Series A Solid Mechanics and Material Engineering*, 47(2), pp. 198-206.

Kim, Y. Y. and Kim, T. S. (2000), Topology optimization of beam cross sections. *International Journal of Solids and Structures*, 37, pp. 477-493.

Liu, S. T., An, X. M. and Jia, H. P. (2007), Topology optimization of beam cross-section considering warping deformation. *Structural and Multidisciplinary Optimization*, 35(5), pp. 403-411.

Luo, Z., Tong, L. Y. and Kang, Z. (2009), A level set method for structural shape and topology optimization using radial basis functions. *Computers & Structures*, 87(7-8), pp. 425-434.

Luo, Z., Wang, M. Y., Wang, S. and Wei, P. (2008), A level set-based parameterization method for structural shape and topology optimization. *International Journal for Numerical Methods in Engineering*, 76(1), pp. 1-26.

Mallat, S. G. (1989), A theory for multiresolution signal decomposition: the wavelet representation. *IEEE Transactions on Pattern Analysis and Machine Intelligence*, 11(7), pp. 674-693.

Patel, N. M., Penninger, C. L. and Renaud, J. E. (2009), Topology optimization for synthesizing extrusion based nonlinear transient designs. *Journal of Mechanical Design*, 131(6), pp. 061003.

Ravnik, J., Škerget, L. and Hriberšek, M. (2004), The wavelet transform for BEM computational fluid dynamics. *Engineering Analysis with Boundary Elements*, 28(11), pp. 1303-1314.

Rozvany, G. I. N. (2008), A critical review of established methods of structural topology optimization. *Structural and Multidisciplinary Optimization*, 37(3), pp. 217-237.

Wang, M. Y., Wang, X. and Guo, D. (2003), A level set method for structural topology optimization. *Computer Methods in Applied Mechanics and Engineering*, 192, pp. 227-246.

Wendland, H. (2006), Computational aspects of radial basis function approximation, Topics in Multivariate Approximation and Interpolation. *Studies in Computational Mathematics*, 12, pp. 231-256.

Zhou, M., Fleury, R., Shyy, Y. K., Thomas, H. L. and Brennan J. M. (2002), Progress in topology optimization with manufacturing constraints. *9th AIAA/ISSMO Symposium on Multidisciplinary Analysis and Optimization*, Atlanta.

Zuberi, R. H., Zuo, Z. X. and Long, K. (2009). Topological optimization of beam cross section by employing extrusion constraint. *ISCMII and EPMESCXII*, Hong Kong-Macau.